Title	Order-to-disorder structural transformation of a coordination polymer and its influence on proton conduction.
Author(s)	Horike, Satoshi; Chen, Wenqian; Itakura, Tomoya; Inukai, Munehiro; Umeyama, Daiki; Asakura, Hiroyuki; Kitagawa, Susumu
Citation	Chemical communications (2014), 50(71): 10241-10243
Issue Date	2014-07-16
URL	http://hdl.handle.net/2433/200183
Right	This journal is © The Royal Society of Chemistry 2014.
Type	Journal Article
Textversion	author

Journal Name

RSCPublishing

COMMUNICATION

Order-to-disorder structural transformation of a coordination polymer and its influence on proton conduction

Cite this: DOI: 10.1039/xoxxoooooox

Satoshi Horike,[a,b] Wenqian Chen,[a] Tomoya Itakura,[c] Munehiro Inukai,[d] Daiki Umeyama,[a] Hiroyuki Asakura[e] and Susumu Kitagawa[a,d]

Received ooth January 2012,
Accepted ooth January 2012

DOI: 10.1039/xoxxoooooox

www.rsc.org/

We observed an ordered-to-disordered structural transformation in a Cu^{2+} coordination polymer and investigated its influence on the proton conductivity. The transformation generated highly mobile proton carriers in the structure. The resulting material exhibited a conductivity greater than 10^{-2} S cm^{-1} at 130 °C. The structural transformation and the conduction mechanism were investigated by EXAFS, TPD-MS and NMR.

In the last decades, much attention has been devoted to coordination polymers (CPs) or metal-organic frameworks (MOFs) composed of metal ions and bridging ligands because of their rich structures and functions.[1-13] Notably, almost all of the reports in the literature focus on crystalline, ordered structures because we can design and discuss close relationships between the crystal structures and functions. However, the literature contains few reports related to amorphous, disordered structures in CP/MOFs.[14, 15] Recently, some interesting observations of crystal-to-amorphous transformations have been reported[16-18] and more unique functions are expected to be derived from disordered systems. In the field of solid state ionics, high ion conductivity is essential in electronics applications and amorphous-state materials often exhibit higher conductivity than their corresponding crystalline state.[19-22] This greater conductivity is observed in both polymer and inorganic electrolytes because the disordered nature results in the generation of concentrated mobile ion carriers in structures. Therefore, the design of structurally disordered CP/MOFs with mobile ion carriers is a promising approach to the preparation of solids with high ion conductivity. In this work, we propose the potential of disordered structures of CP/MOFs to possess fast proton (H^+) conduction path. Transformation from ordered to disordered structures was induced by heating microcrystals, and the disordered state exhibits H^+ conductivity 10^4 times greater than that of the crystalline state.

We employed $[ImH_2][Cu(H_2PO_4)_2Cl]\cdot H_2O$ (denoted as **1**, ImH_2 = protonated imidazole) as a starting compound.[23] The crystal structure of **1** is shown in Figure 1; it has two crystallographically independent Cu^{2+} and $H_2PO_4^-$ ions and one independent Cl^- ion. Both Cu^{2+} ions possess octahedral coordination geometry. Four oxygen atoms from the phosphate groups and two Cl^- ions coordinate to the Cu^{2+} centres to forms 1-D chains with a formula of $[Cu(H_2PO_4)_2Cl]^-$ along the *b* axis. Each phosphate coordinates to Cu^{2+} in both monodentate and bidentate fashion. The protonated imidazole (ImH_2) and the water molecule are located in interspaces of the anionic 1-D chains running along the *b* axis. The guest water forms multiple hydrogen bonds between O atoms of phosphates from two neighbouring 1-D chains, and it stabilises the alignments of the 1-D chains via H-bonds.

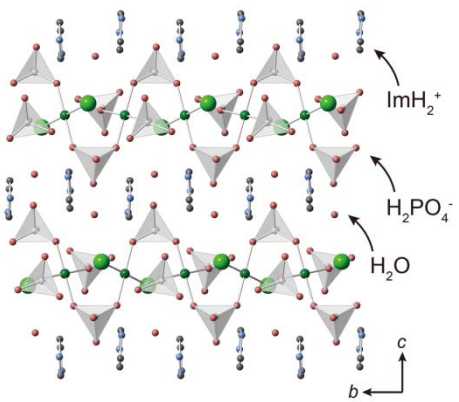

Figure 1. Crystal structure of **1** at −50 °C. Grey, skyblue, pink, deep-green, light-grey and light-green represent C, N, O, Cu, P and Cl atoms, respectively. Guest water molecules are omitted. PO_4 are displayed as polyhedra.

We synthesised microcrystalline powder of **1** by mechanical milling a mixture of $CuCl_2$, phosphoric acid and imidazole. The as-synthesised powder of **1** was washed with ethanol and subsequently dried under a N_2 atmosphere. The X-ray powder diffraction (XRPD) pattern of the powdered sample at 25 °C (Figure 2a) matches the pattern simulated from the single-crystal structural data. We attempted to remove the intercalated water to reduce the long-range order in the structure. Thermogravimetric analysis (TGA) of **1** shows a weight loss of 6 wt% at 100–120 °C; this weight loss corresponds to the release of the guest water molecule in **1** (calculated weight loss is 6 wt%). We then heated **1** at 130 °C for 6 h under vacuum and

obtained dehydrated **1** (hereafter denoted it as **1′**). Figure 2 shows the XRPD pattern of **1′**, which is different from that of **1**; the XRPD pattern of **1′** indicates it is highly disordered. The TGA profile of **1′** shows no clear weight loss at temperatures less than 180 °C.

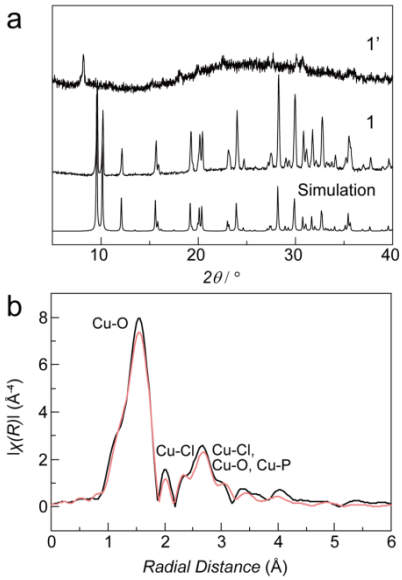

Figure 2. (a) X-ray powder diffraction (XRPD) patterns of **1** and **1′** at 25 °C. The pattern simulated from single-crystal structural data is also shown. (b) Radius distribution functions (RDFs) of the Fourier-transformed Cu K-edge EXAFS spectra for **1** (black) and **1′** (pink) at 25 °C.

Figure 3a shows Arrhenius plots of the H^+ conductivity of **1** and **1′** under a N_2 atmosphere (zero-humidity conditions); the measurements were performed on pelletized samples. Because **1** starts to release its crystalline water above 70 °C, we show the conductivity in the range of 25 to 70 °C. **1** exhibits negligible conductivities (1×10^{-11} S cm^{-1} at 25 °C and 4×10^{-11} S cm^{-1} at 70 °C). The crystal structure of **1** contains numerous hydrogen bonds between the anionic 1-D chains, the guest water molecules and the ImH_2 ions; these bonds stabilise the H^+ in the structure, which results in low H^+ conductivity. The localised water in the crystal structure does not contribute to the H^+ conductivity because of its low mobility. However, **1′** exhibits a conductivity of 2×10^{-7} S cm^{-1} at 25 °C (Figure 3b), and the conductivity increases upon heating to 2×10^{-2} S cm^{-1} at 130 °C (Figure 3c). The conductivity of **1′** is 10^6 times higher than that of **1** at 70 °C. The activation energy of this conductivity is 1.1 eV, which indicates that both Grotthus- and vehicle-type hopping mechanisms contribute to the H^+ conductivity in **1′**.[24] The observed H^+ conductivity of **1′** at 130 °C is regarded as one of the highest among the known solid anhydrous H^+ conductors such as solid acids[25] and phosphoric-acid-doped polybenzimidazole.[26, 27]

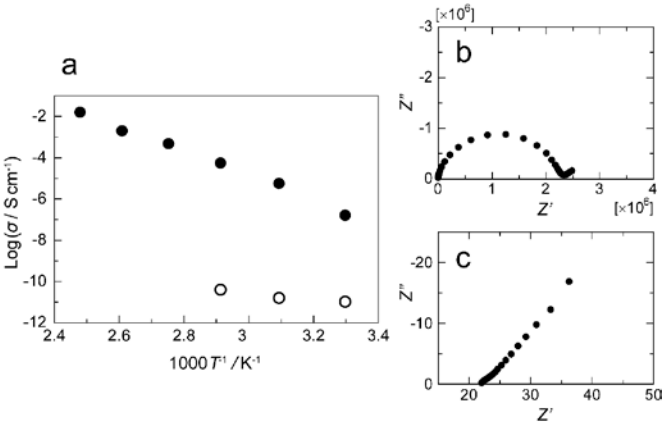

Figure 3. Arrhenius plots of the H^+ conductivity of **1** (open circles) and **1′** (solid circles) under a N_2 atmosphere. Nyquist plots of **1′** at (b) 30 °C and (c) 130 °C; the pellet thickness is 0.69 mm.

We characterised the origin of the high H^+ conductivity in **1′**. The N–H stretching peaks of the imidazole in the IR spectrum in **1′** suggest that the imidazole moieties in **1′** are all protonated (ImH_2 form).[28, 29] This result indicates that deprotonation of ImH_2 does not occur via the transformation of **1** to **1′**. To study the local coordination environment of the Cu ions in **1** and **1′**, we conducted extended X-ray absorption fine structure (EXAFS) measurements.[30] Pseudo radial distribution functions (RDFs) of the Fourier-transformed Cu K-edge EXAFS spectra of **1** and **1′** are shown in Figure 2b. We first performed an FEFF simulation for **1** using its single-crystal XRD data;[31, 32] the peaks appearing at 1.55 and 2.0 Å were assigned to Cu–O and Cu–Cl, respectively. The broader peak at 2.7 Å includes Cu–Cl, Cu–O and Cu–P. The observed RDF patterns of **1** and **1′** are similar, which indicates that the local coordination geometry of Cu^{2+} is unchanged during the structural transformation. Meanwhile, these assigned peaks in the spectrum of **1′** are slightly less intense than those in the spectrum of **1**, which suggests that either the coordination number around Cu^{2+} decreased or the Debye–Waller factors increased as a consequence of the statistical disordering of the local atomic distribution. To investigate the transformation from **1** to **1′**, we performed TPD-MS analyses of the samples under a N_2 atmosphere. We first observed the release of intercalated water at 80–120 °C, as previously described. Interestingly, we then observed the release of HCl from 90 to 130 °C. The Cl^- ions of HCl originate from the bridging Cl^-, and the H^+ of HCl originates from either the $H_2PO_4^-$ or ImH_2 moieties in **1** (Figure 1). The distorted coordination geometry of Cu^{2+} facilitates the reaction of Cl^- with the acidic proton. The ImH_2 ions remain, even at 200 °C. As a result, we suggest that the mechanism of the transformation from **1** to **1′** is as follows. Guest water molecules in **1** are released at 100 °C, and the structure loses its long-range order; gaseous HCl is formed by the reaction between $H_2PO_4^-$ groups and neighbouring Cl^- groups in the chains at temperatures below 130 °C. Not all of the Cl^- ions in **1** are used to generate HCl, as confirmed by EXAFS, and half of the Cl^- ions retain their coordination bond with Cu^{2+} in **1′** according to the elemental analysis results. The transformation in the formula of **1** to that of **1′** is proposed as follows:

$$[ImH_2][Cu(H_2PO_4)_2 \cdot Cl] \cdot H_2O \rightarrow [ImH_2][Cu(H_2PO_4)_{1.5}(HPO_4)_{0.5} \cdot Cl_{0.5}]$$

One of the factors necessary for high ion conductivity in disordered states is the enhanced mobility of ion carriers. To investigate the

dynamics of H^+ carriers in **1** and **1′**, we collected variable-temperature solid-state ^2H NMR spectra of deuterated samples of **1** and **1′** (Figure 4). We synthesised **1** and **1′** using imidazole-D4 and monitored the dynamics of imidazolium cation-D4 (ImD_2) in the structures. These structures are identical to those of the protonated **1** and **1′** determined by XRPD. The spectrum of deuterated **1** shows a broad peak, even at 80 °C (Figure 4a), which suggests that ImD_2 exhibits poor mobility; the sharp peak at 0 ppm in the spectrum of deuterated **1′** in Figure 4b corresponds to the highly mobile ImD_2 species.[33-35] The transformation from **1** to **1′** breaks the H-bonds and generates the mobile ImH_2 ions as H^+ carriers.

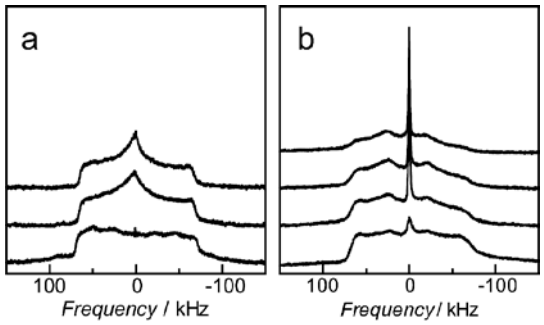

Figure 4. Variable-temperature solid-state ^2H NMR of (a) **1** and (b) **1′**, both of which were synthesised using imidazole-D4. From bottom to top: 25 °C, 40 °C, 60 °C (for **1** and **1′**) and 80 °C (only for **1′**).

Conclusions

We induced the structural transformation of a Cu^{2+} coordination polymer from an ordered crystalline state to a disordered state using a heating process. The disordered state contains highly mobile H^+ carriers, which results in a H^+ conductivity under anhydrous conditions of 2×10^{-2} S cm^{-1} at 130 °C, which is substantially higher than the conductivity of the ordered state. This conductivity is one of the highest values reported among the family of solid-state H^+ conductors in this temperature range. PXRD, EXAFS, TPD-MS and solid-state ^2H NMR studies revealed the mechanisms of the transformation and the fast H^+ conduction. The results highlight the superior potentials of disordered structures of CP/MOF for materials of solid state ionics.

The EXAFS experiments were conducted at the BL5S1 of Aichi Synchrotron Radiation Center. This work was supported by the PRESTO and A-STEP programs of the Japan Science and Technology Agency (JST), and a Grant-in-Aid for Scientific Research on the Innovative Areas: “Fusion Materials” and Grant-in-Aid for Young Scientists (A) from the Ministry of Education, Culture, Sports, Science and Technology, Japan.

Notes and references

[a] Department of Synthetic Chemistry and Biological Chemistry, Graduate School of Engineering, Kyoto University, Katsura, Nishikyo-ku, Kyoto 615-8510, Japan

[b] Japan Science and Technology Agency, PRESTO, 4-1-8 Honcho, Kawaguchi, Saitama 332-0012, Japan

[c] DENSO CORPORATION, 1-1, Showa-cho, Kariya, Aichi 448-8661, Japan

[d] Institute for Integrated Cell-Material Sciences (WPI-iCeMS), Kyoto University, Yoshida, Sakyo-ku, Kyoto 606-8501, Japan

[e] Synchrotron Radiation Research Center, Nagoya University, Furo-cho, Chikusa, Nagoya 464-8603, Japan

† Electronic Supplementary Information (ESI) available: [Experimental procedures, XRD, TGA, IR, TPD-MS, Elemental analysis]. See DOI: 10.1039/c000000x/

1. A. K. Cheetham, G. Férey and T. Loiseau, *Angew. Chem. Int. Ed.*, 1999, **38**, 3268-3292.
2. O. M. Yaghi, M. O'Keeffe, N. W. Ockwig, H. K. Chae, M. Eddaoudi and J. Kim, *Nature*, 2003, **423**, 705-714.
3. M. J. Rosseinsky, *Micropor. Mesopor. Mater.*, 2004, **73**, 15-30.
4. S. Kitagawa, R. Kitaura and S. Noro, *Angew. Chem. Int. Ed.*, 2004, **43**, 2334-2375.
5. G. Férey, *Chem. Soc. Rev.*, 2008, **37**, 191-214.
6. G. K. Shimizu, R. Vaidhyanathan and J. M. Taylor, *Chem. Soc. Rev.*, 2009, **38**, 1430-1449.
7. A. Betard and R. A. Fischer, *Chem. Rev.*, 2012, **112**, 1055-1083.
8. D. M. D'Alessandro, B. Smit and J. R. Long, *Angew. Chem. Int. Ed.*, 2010, **49**, 6058-6082.
9. L. E. Kreno, K. Leong, O. K. Farha, M. Allendorf, R. P. Van Duyne and J. T. Hupp, *Chem. Rev.*, 2012, **112**, 1105-1125.
10. K. J. Gagnon, H. P. Perry and A. Clearfield, *Chem. Rev.*, 2012, **112**, 1034-1054.
11. M. Yoon, K. Suh, S. Natarajan and K. Kim, *Angew. Chem. Int. Ed.*, 2013, **52**, 2688-2700.
12. S.-L. Li and Q. Xu, *Energy. Environ. Sci.*, 2013, **6**, 1656-1683.
13. T. Yamada, K. Otsubo, R. Makiura and H. Kitagawa, *Chem. Soc. Rev.*, 2013, **42**, 6655-6669.
14. A. B. Cairns and A. L. Goodwin, *Chem. Soc. Rev.*, 2013, **42**, 4881-4893.
15. T. D. Bennett and A. K. Cheetham, *Acc. Chem. Res.*, 2014, **47**, 1555-1562.
16. K. W. Chapman, G. J. Halder and P. J. Chupas, *J. Am. Chem. Soc.*, 2009, **131**, 17546-17547.
17. Y. H. Hu and L. Zhang, *Phys. Rev. B*, 2010, **81**, 1741031-1741035.
18. A. U. Ortiz, A. Boutin, A. H. Fuchs and F.-X. Coudert, *J. Phys. Chem. Lett.*, 2013, **4**, 1861-1865.
19. T. Minami, *J. Non-Cryst. Solids*, 1985, **73**, 273-284.
20. C. A. Angell, *Ann. Rev. Phys. Chem.*, 1992, **43**, 693-717.
21. J. Y. Song, Y. Y. Wang and C. C. Wan, *J. Power Sources*, 1999, **77**, 183-197.
22. J. C. Dyre, P. Maass, B. Roling and D. L. Sidebottom, *Rep. Prog. Phys.*, 2009, **72**, 046501.
23. S. Neeraj, T. Loiseau, C. N. R. Rao and A. K. Cheetham, *Solid State Sci.*, 2004, **6**, 1169-1173.
24. K. D. Kreuer, *Chem. Mater.*, 1996, **8**, 610-641.
25. A. Goni-Urtiaga, D. Presvytes and K. Scott, *Int. J. Hydrog. Energy*, 2012, **37**, 3358-3372.
26. J. Wainright, J. T. Wang, D. Weng, R. Savinell and M. Litt, *J. Electrochem. Soc.*, 1995, **142**, L121-L123.
27. X. Glipa, B. Bonnet, B. Mula, D. J. Jones and J. Rozière, *J. Mater. Chem.*, 1999, **9**, 3045-3049.
28. M. Nakayama, Y. Sugiura, T. Hayakawa and M. Nogami, *Phys. Chem. Chem. Phys.*, 2011, **13**, 9439-9444.
29. S. Horike, D. Umeyama, M. Inukai, T. Itakura and S. Kitagawa, *J. Am. Chem. Soc.*, 2012, **134**, 7612-7615.
30. D. E. Sayers, E. A. Stern and F. W. Lytle, *Phys. Rev. Lett.*, 1971, **27**, 1204.
31. B. Ravel and M. Newville, *J. Synchrotron Radiat.*, 2005, **12**, 537-541.
32. J. J. Rehr, J. J. Kas, F. D. Vila, M. P. Prange and K. Jorissen, *Phys. Chem. Chem. Phys.*, 2010, **12**, 5503-5513.
33. J. A. Hurd, R. Vaidhyanathan, V. Thangadurai, C. I. Ratcliffe, I. L. Moudrakovski and G. K. Shimizu, *Nat. Chem.*, 2009, **1**, 705-710.
34. S. Bureekaew, S. Horike, M. Higuchi, M. Mizuno, T. Kawamura, D. Tanaka, N. Yanai and S. Kitagawa, *Nat. Mater.*, 2009, **8**, 831-836.

35. S. Horike, D. Umeyama and S. Kitagawa, *Acc. Chem. Res.*, 2013, **46**, 2376-2384.

